Pointing-dependent Variation of a Radio Telescope Reference Point – First Investigation at the Onsala Space Observatory

Pointing-dependent Variation of a Radio Telescope Reference Point – First Investigation at the Onsala Space Observatory

Ausrichtungsabhängige Variation eines Radioteleskopreferenzpunkts – erste Untersuchung am Onsala Space Observatory

Michael Lösler | Cornelia Eschelbach | Rüdiger Haas

Summary

The International Terrestrial Reference Frame (ITRF) is a highly accurate realisation of the International Terrestrial Reference System (ITRS), an Earth-fixed global geodetic reference system. It forms the backbone for almost all scientific investigations of the dynamic system Earth and is realised through the combination of several space-geodetic techniques. The positions of geometric reference points of these space-geodetic techniques, such as radio telescopes used for very long baseline interferometry (VLBI), are the physical realisation of the frame on Earth. The precision and the reliability of such a reference frame depend on the spatio-temporal stability of the involved reference points defining the datum. In this contribution, the reference point stability of a modern VGOS radio telescope at the Onsala Space Observatory is investigated. The aim is to quantify the magnitude of changes, especially when the radio telescope rotates about the azimuth and elevation axes, and to identify a suitable location for permanent monitoring instrumentation to monitor the spatio-temporal variation of the reference point position. Based on measurements with a highly precise laser tracker, horizontal and vertical variations were detected. The horizontal variations of approximately ±250 µm indicate a slightly asymmetrical arrangement of the telescope components. The vertical variations of about ±15 µm are quite small and indicate minor deviations in the construction work of the radio telescope.

Keywords: radio telescope, reference point, monitoring, laser tracker, VGOS, Onsala Space Observatory

Zusammenfassung

Der Internationale Terrestrische Referenzrahmen (ITRF) ist eine hochgenaue Realisierung des Internationalen Terrestrischen Referenzsystems (ITRS), ein erdfestes globales geodätisches Referenzsystem. Es bildet die fundamentale Basis für nahezu alle wissenschaftlichen Untersuchungen des dynamischen Systems Erde und wird durch die Kombination mehrerer geodätischer Raumverfahren gewonnen. Die Positionen der geometrischen Bezugspunkte dieser Raumverfahren, wie z. B. Radioteleskope, die für die Radiointerferometrie auf langen Basen (VLBI) verwendet werden, bilden die physische Realisierung des Referenzsystems auf der Erde. Die Genauigkeit und die Zuverlässigkeit eines solchen Bezugsrahmens hängen von der räumlichen und zeitlichen Stabilität der verwendeten Referenzpunkte ab, die das Datum definieren. In diesem Beitrag wird die Referenzpunktstabilität eines modernen VGOS-Radioteleskops am Onsala Space Observatory untersucht. Ziel dieser Untersuchung ist es, vertikale, aber auch horizontale Änderungen zu quantifizieren, insbesondere bei Rotation des Radioteleskops um die Azimut- und Elevationsachse, und einen geeigneten Standort für ein festinstalliertes Messsystem zur Überwachung der raum-zeitlichen Variation der Referenzpunktposition zu identifizieren. Mit einem hochpräzisen Lasertracker konnten sowohl horizontale als auch vertikale Schwankungen nachgewiesen werden. Während die horizontalen Schwankungen von etwa ±250 µm vermutlich auf eine leicht asymmetrische Anordnung einzelner Teleskopkomponenten zurückzuführen sind, deuten die geringen vertikalen Schwankungen von etwa ±15 µm auf kleine Abweichungen bei der Konstruktion des Radioteleskops hin.

Schlüsselwörter: *Radioteleskop, Referenzpunkt, Monitoring, Lasertracker, VGOS, Onsala Space Observatory*

1 Introduction

The United Nations General Assembly adopted in February 2015 the resolution "A Global Geodetic Reference Framework for Sustainable Development" (A/RES/69/266, United Nations (2015)) which highlights the importance of global geodetic measurements for a sustainable development of society. The terrestrial part of the Global Geodetic Reference Framework (GGRF) is realised by the International Terrestrial Reference Frame (ITRF), and the last realisation is the ITRF2020 (Altamimi et al. 2023). The ITRF is based on observations with a multitude of instrumentation for space-geodetic measurements. One of these techniques is very long baseline interferometry (VLBI), which makes use of radio telescopes to observe extragalactic radio sources in the international celestial reference frame (ICRF) (e. g. Sovers et al. 1998, Charlot et al. 2020). The VLBI observations are coordinated internationally in the observing program of the International VLBI Service for Geodesy and Astrometry (IVS) (cf. Nothnagel et al. 2017). The terrestrial reference of VLBI observations are the reference points of the radio telescopes, which are geometrically defined as the

DOI 10.12902/zfv-0524-2025

orthogonal projection of the secondary axis onto the primary axis. For the next generation VLBI system, called VLBI Global Observing System, a requirement for the three-dimensional stability of 0.3 mm in a root-mean-square sense was requested by Petrachenko et al. (2009, p. 25), to reach the 1 mm accuracy goal in the position on a global scale aimed by the Global Geodetic Observing System (cf. Gross et al. 2009). Since for example temperature induced deformations are expected as discussed by Wresnik et al. (2006), the monitoring of the spatio-temporal reference point stability with e. g. invar measurement systems was suggested. Beside vertical variations caused by temperature changes, any elevation-dependent changes, such as the inclination of the radio telescope, would also affect the reference point position and limit the pointing accuracy of the telescope. It is thus of interest to study how such measurement systems can be integrated in the modern VGOS radio telescopes, such as the VGOS twin telescopes at the Onsala Space Observatory (Haas et al. 2019).

Section 2 deals with the measurement concept performed at the Onsala Space Observatory. A highly precise laser tracker AT960 observed targets close to the reference point position. Due to the limited space inside the radio telescope under investigation, the targets were observed via a plane mirror. The analysis and the results are discussed in Section 3. In order to quantify the magnitude of changes and to identify a suitable location for a permanently installed measurement system to monitor the spatio-temporal variation of the reference point position, the analysis was separated into the horizontal and the vertical component. The vertical variation is studied in Section 3.1, and in Section 3.2 the horizontal variation is investigated. Additionally performed inclination measurements are addressed in Section 3.3. Finally, Section 4 concludes this contribution.

2 Measurement Concept

VLBI radio telescopes observe quasi-stellar objects distributed in different directions in space and consist of a primary and a secondary axis of rotation. For an azimuth-elevation-type radio telescope, the primary and the secondary axes correspond to the azimuth and the elevation axes. The arrangement of the axes is similar to that of a theodolite. The geometric reference point of a VLBI radio telescope results from the orthogonal projection of the secondary axis onto the primary axis (e. g. Lösler 2009, Ning et al. 2015). The reference point is geometrically defined and often referred to as invariant point, because its position is independent of the pointing direction of the telescope (cf. Lösler et al. 2021). However, the reference point is typically not realised within the radio telescope construction and a direct observation is impossible. Various indirect approaches have been developed to determine the position of the reference point (Lösler 2021, p. 63 ff). Almost all approaches require observed targets in different telescope orientations. These targets are mounted at rotatable construction elements of the radio telescope, and the reference point is derived from the resulting trajectories of these targets (e. g. Li et al. 2013, Lösler et al. 2013, Guillory et al. 2023). As each target position uniquely depends on the telescope orientation, these approaches are almost insensitive to detect pointing-dependent variation of the reference point. Small deviations are masked by the large number of observations. To detect these small deviations, specific measurement concepts are recommended that observe the desired quantity almost directly. As the reference point is not physically realised, the challenge is to find a suitable substitute location for a representative monitoring of reference point's variation.

In order to quantify the magnitude of pointing-dependent variation as well as to identify a suitable location for a permanently installed monitoring system inside the Onsala Twin Telescopes, a measurement campaign was carried out at the Onsala Space Observatory in 2023. As both radio telescopes are identical in construction, we restrict ourselves to the results obtained from the south-western radio telescope with DOMES 10402S015. The main reflector diameter is 13.2 m and the height of the elevation axis is about 10.5 m above the ground. The azimuth axis is realised by a conical hollow tube. The tube is permanently mounted on the concrete foundation of the radio telescope and, therefore, is independent of the pointing direction of the radio telescope. The length of the tube is about $h_E = 9$ m, and consists of several tapering cylindrical segments. The first segment at the ground floor has a diameter of about 60 cm. The diameter of the last segment at the top of the tube is 3.5 cm. The tube is a non-structural component and realises the ground-fixed part of the azimuth encoder, which is located at the end of the tube. The counterpart of the encoder is mounted on the co-rotating azimuth cabin. The end of the tube is the highest position above the ground level, which is independent of the telescope's pointing direction and is closest to the reference point. It is intended for the installation of sensors for an almost direct monitoring of vertical changes of the reference point. Whether this position is also suitable for monitoring of horizontal variation is one of the subjects of this investigation. Hereinafter, this position is denoted by **E**, and depicted in Fig. 1.

Hexagon's laser tracker AT960 was used to evaluate the substitute location for a permanently installed measurement system for monitoring both vertical and horizontal variations. According to ISO 10360-10 (2021), the manufacture specifies the maximum permissible error (MPE) of a three-dimensional position by $15\ \mu m + 6\ \frac{\mu m}{m}$. As the MPE of the absolute interferometer is specified by $0.5\ \frac{\mu m}{m}$, the uncertainty of a three-dimensional position is mainly affected by the angular measurements. For a position at a distance of 10 m, the MPE is less than 100 µm, which is sufficient as the requirement for VGOS radio telescopes strives for an accuracy of 300 µm in the reference point position (cf. Petrachenko et al. 2009, p. 25).

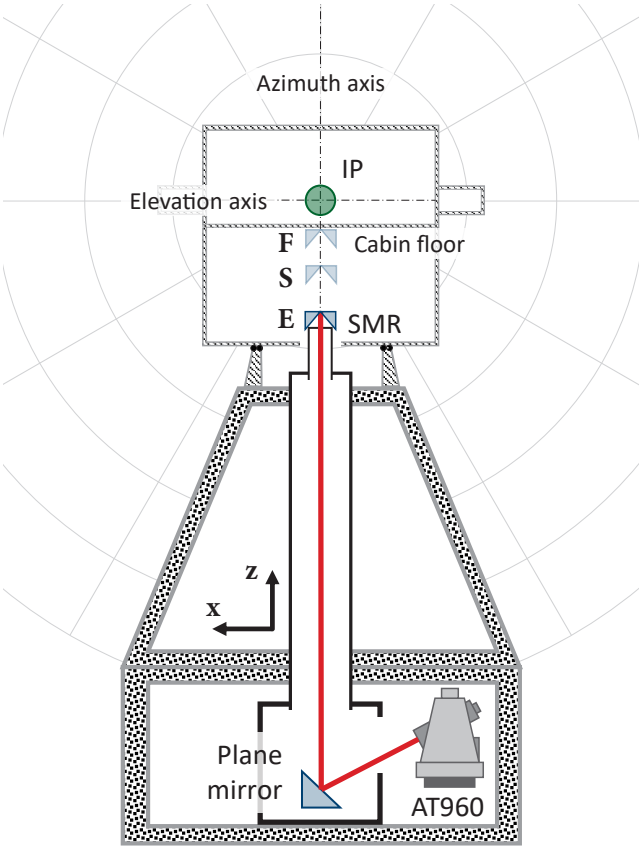

Fig. 1: Schematic representation of the realised measurement configuration. The laser beam of the AT960 laser tracker is deflected onto the SMR at a plane mirror. The SMR was either positioned at the end of the tube **E**, at the support elements of the cabin **S**, or at the cabin floor **F** close to the invariant point denoted by IP.

Due to the small diameter of the tube's top segment, a downwards pointing 1.5″ spherically mounted reflector (SMR) is placed at the end of the tube **E**. Two further SMR positions were realised by temporarily mounted drift-nests. The first one at supporting elements **S** on the cabin, and the second one at the cabin floor **F**. Whereas the position **E** is rotational invariant, **S** and **F** co-rotate with the radio telescope in azimuth. On the ground floor, the tube has two side openings, each with a diameter of 35 cm. These openings are designed for the installation of measuring devices inside the hollow tube. Due to the dimension of the AT960 laser tracker, the instrument could not be positioned inside the tube to measure the SMR directly. For that reason, a plane mirror was placed inside the tube, and the SMR was observed by the instrument via the mirror. Plane mirrors are frequently used in metrology applications to increase the field of view of photogrammetric camera systems (Hesch et al. 2008). Morse and Welty (2015) included a plane mirror in a dynamic test procedure to evaluate the performance of laser trackers. Moreover, plane mirrors are used for optical alignments in industrial applications (Burge et al. 2007). In general, plane mirrors extend the working range of optical instruments and fit the measuring systems to the available space.

Fig. 1 depicts the performed measurement configuration, when the laser tracker was placed outside the tube. A plane mirror inside the tube deflects the AT960 laser beam onto the SMR. In order to optimally align the laser beam onto the SMR, the tiltable plane mirror was mounted on a cross slide, as shown in Fig. 2. The tilting axis of the plane mirror was perpendicular to the laser beam of the AT960. The SMR was either positioned at the end of the tube **E**, at the supporting elements on the cabin **S**, or at the cabin floor **F**. All SMR positions were close to the azimuth axis, and were observable in a unified frame without changing the configuration of the instrument and the mirror. Therefore, stationing uncertainties do not occur. Due to the high-precision distance measurement, the configuration is particularly sensitive to detect vertical variation. However, the uncertainty of the horizontal variation is mainly limited by the angle measurements. The dimension of the tube limits the deviation between the deflected laser beam and the azimuth axis. The maximum misalignment is $\theta = 2°$. A true displacement of 1 mm in the spatial position would cause an error of about $h_E(1 - \cos(\theta)) = 0.5$ µm. This error is negligible if the plane mirror and the deflected laser beam are almost centred in the tube. The meteorological environmental parameters were assumed to be stable because the radio telescope is equipped with an air conditioning system. Temperature, air pressure, and humidity were measured by an external meteorological station, and corrections were applied to the observed distances. The instruments were switched on and warmed up for about 12 h, to avoid measurement drifts caused for instance by heating effects of instrument components (cf. Gassner and Ruland 2011, Pérez Muñoz et al. 2016).

The radio telescope was rotated in predefined azimuth and elevation positions to observe pointing-dependent variation. Specific experiments were performed within the full working range between –90° and 540° in azimuth, using an azimuth step-size of $\Delta\alpha = 15°$. These azimuth-dependent experiments were carried out using elevation angles ε of 5°, 45° and 90°. Verification measurements were restricted to

Fig. 2: Laser tracker AT960 in front of the side opening of the tube. An SMR is observed via a plane mirror located centrally inside the tube. The plane mirror is mounted on a cross slide and shown in detail.

the range between 0° and 360°. In order to evaluate elevation-depended variation, the radio telescope was rotated about the elevation axis in steps of $\Delta\varepsilon$ = 10° from 10° to 90° as well as 5°. These elevation-dependent experiments were repeated at 0°, 90°, 180° and 270° in azimuth. The measurement time for a single position, including the rotation of the radio telescope, took about 30 s, resulting in a total measurement time of an experiment of less than 20 min. Even though the measurement time was quite short and the radio telescope is equipped with an air conditioning system, a temperature-induced expansion of the monument during the experiment cannot be completely excluded, and a trend in the series must be considered during the data analysis as proposed by Foppe and Neitzel (2014).

3 Analysis and Results

The analysis of the data and the obtained results are described in detail in the following subsections. The aim of this investigation is to quantify the magnitude of changes, especially when the radio telescope rotates about the azimuth and elevation axes, and to identify a suitable location for permanent monitoring instrumentation to monitor the spatio-temporal variation of the reference point position. Whereas vertical variation is investigated in Section 3.1, Section 3.2 deals with the analysis of the horizontal variation. In order to verify the detected changes, additional inclination measurements were performed. The analysis and the results are discussed in Section 3.3.

3.1 Vertical Variation

As shown in Fig. 1, the measured distances s of the AT960 correspond to the z-component and a change in the distance relates to a change of the height, i. e.,

$$\Delta z_i \approx \Delta s_i . \tag{1}$$

The vertical variation Δz_i observed at the end of the tube **E** while the radio telescope was rotated about the azimuth axis is depicted in Fig. 3a for the three elevation angles 5°, 45° and 90°. The vertical variation is quite small and lies in a range of about ±15 µm. The pattern is independent of the elevation angle under investigation and is confirmed by the elevation-dependent experiments. The correlation coefficients are greater than 96 % and illustrate the strong dependencies between the three series. The cyclical signal is overlaid by a slight drift, which indicates a small thermal expansion of the radio telescope during the measurements.

In order to verify the vertical variation observed at the end of the tube, the experiments were repeated using the SMR position **F** at the cabin floor and partially at the support elements **S**, cf. Fig. 1. Fig. 3b depicts the vertical variation Δz_i observed at the cabin floor and confirms the measurements at the end of the tube. The small deviations between the measurement series in Fig. 3a and Fig. 3b indicate a small component-specific variation, such as a minor structural deformation of the cabin floor. Nevertheless, the striking cyclical signal is clearly recognisable at both positions. The experiment at SMR position **S** was restricted to the azimuth range from 0° to 360° as well as ε = 90°, because the cyclical pattern has already been confirmed by this series, cf. Fig. 3c.

The observed vertical variation appears to be independent of elevation position. For that reason, the variation cannot be explained by changing load cases caused by different pointing directions. More likely is an unevenness of the gear rim realising the circular azimuth track, which is mounted on the top of the concrete monument. Track unevenness was also detected by inclination measurements at large radio telescopes such as the 100 m Qi Tai Telescope (Li et al. 2022) and the 25 m Nanshan Radio Telescope (Xu et al. 2023), and leads to a deterioration of the antenna's pointing accuracy (Gawronski et al. 2000, Li et al. 2017). However, regardless of the reason, the vertical variation is repeatable, systematic, and correctable. According to Foppe and Neitzel (2014), a suitable function reads

$$\Delta z(\alpha) = n_i + m_i\,\alpha + \sum_{j\in\mathcal{J}} a_j \cos\left(\frac{2\pi j}{T}\alpha + b_j\right), \tag{2}$$

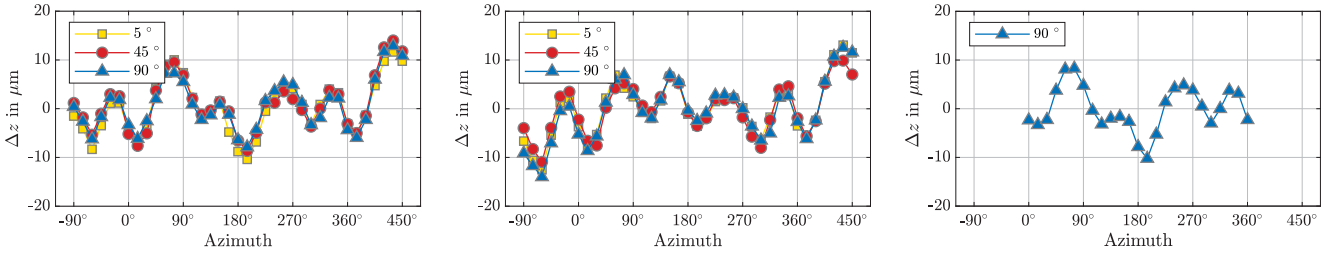

(a) Position **E** (b) Position **F** (c) Position **S**

Fig. 3: Vertical variation observed at different SMR positions: (a) the end of the tube, (b) at the cabin floor and (c) at the support elements on the cabin, while the radio telescope was rotated about the azimuth axis in fixed elevations. Yellow squares, red circles, and blue triangles relate to the measurement series in elevation 5°, 45° and 90°. Please note, the verification position **S** was only observed between 0° and 90° in azimuth, while **E** and **F** were observed from –90° to 450°.

Tab. 1: Estimated coefficients and related standard deviations of the derived correction model

j	a in µm	σ_a in µm	b in °	σ_b in °
1	2.5	0.4	70.9	7.8
2	3.2	0.3	163.5	6.1
4	4.6	0.3	–93.9	4.0

where $\mathcal{J}$ is an index set of the dominant series terms, which are derived by e. g. an amplitude spectrum of a Fourier series (e. g. Heunecke et al. 2013). The second term in (2) parameterises the cyclic part of the series and is known as amplitude-phase form. The amplitude is a_j, the phase angle is b_j, and $T := 360°$ denotes the period. To reduce a drift in the i-th series, the expression is extended by the first term, which represents the linear function of a straight line with parameters n_i and m_i. By considering only the dominant series terms in $\mathcal{J}$, the unknown coefficients n_i, m_i, a_j, b_j are obtained by means of parameter estimation (Lösler et al. 2010).

Based on the amplitude spectrum, the dominant series terms $\mathcal{J} = \{1,2,4\}$ were derived and introduced to the least-squares adjustment. Tab. 1 summarises the estimated parameters as well as the related standard deviations. The coefficients of the linear part are omitted because only the cyclic part is required for a correction model. The resulting correction function is depicted in Fig. 4. The thermal expansion of the radio telescope is already compensated in VLBI data analysis (Wresnik et al. 2006) or in the framework of reference point determination (Lösler et al. 2016). As the observed variation acts similar to the vertical component of the reference point, the derived correction model can easily be applied in existing software packages to reduce the impact of the systematic vertical variation.

However, compared with the thermal expansion of the radio telescope as a result of daily or seasonal temperature changes, the observed vertical variation is only a second-order effect. Fig. 5 depicts the multi-day vertical variation and the corresponding monument temperature. Although the radio telescope is equipped with an air conditioning system, changes of about 100 µm can be observed within a single day. The correlation coefficient between the temperature and the vertical variation is 96 %. Moreover, seasonal vertical changes are an order of magnitude greater. For instance, Elgered and Carlsson (1995) observed variation between the summer and the winter of 3 mm for the radome-enclosed 20 m VLBI radio telescope at the Onsala Space Observatory. Similar results were also reported by Zernecke (1999) and Mähler et al. (2019) for VLBI radio telescopes at the Geodetic Observatory Wettzell.

Nevertheless, the measurement series at the end of the tube are almost identical with the series obtained at the co-rotating cabin. The position at the end of the tube is sensitive to systematic vertical variation caused by minor

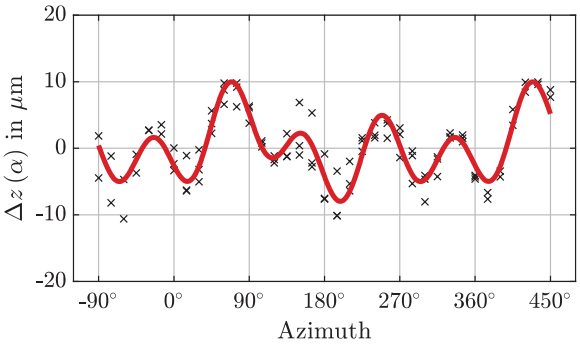

Fig. 4: Derived correction model (red) and averaged sampling points of the three series (black crosses).

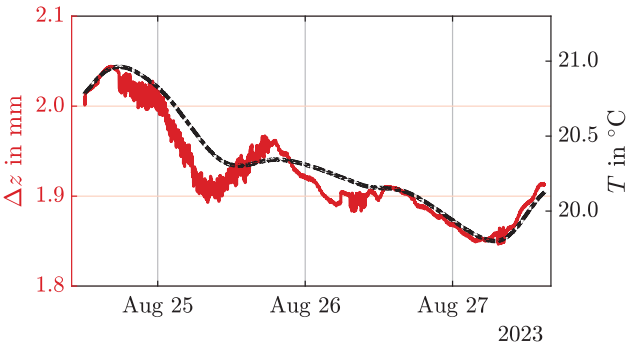

Fig. 5: Multi-day monitoring of the SMR position E using the laser tracker AT960. The vertical variation is shown in red, and the corresponding monument temperature is shown in black.

deviations in the telescope's structure and by temperature changes. Therefore, the position is recommended for a permanently installed measurement system for monitoring vertical changes.

3.2 Horizontal Variation

In contrast to the vertical variation, which directly results from the distance measurement, the horizontal variation mainly relates to the angle measurements. For a straightforward interpretation of the results, a Cartesian representation is advisable. Due to the measurement configuration, changes in the x-component directly relate to the vertical angle ξ and are readily obtained from

$$\Delta x_i = -s_i \sin\left(\Delta\xi_i\right). \tag{3}$$

Here, s_i denotes the slope distance, and $\Delta\xi_i = \xi_i - \overline{\xi}$ is the change of the vertical angle ξ_i w. r. t. the series average $\overline{\xi}$. A change in the y-component corresponds to the direction τ via

$$\Delta y_i = -s_i^{\mathrm{H}} \sin\left(\Delta\tau_i\right), \tag{4}$$

where $s_i^{\mathrm{H}} = s_i \sin\left(\xi_i\right)$ is the horizontal distance, and $\Delta\tau_i = \tau_i - \overline{\tau}$ is the change in the direction measurement τ_i w. r. t. the series average $\overline{\tau}$. As only small angular changes

are to be expected, the horizontal changes Δx and Δy can be sufficiently approximated by the arc length formula, i. e.,

$$\Delta x_i \approx -s_i \Delta \xi_i \tag{5}$$

$$\Delta y_i \approx -s_i^{\mathrm{H}} \Delta \tau_i, \tag{6}$$

where $\Delta\xi_i$ and $\Delta\tau_i$ are the central angles, respectively.

Elevation-dependent deformation at the receiving unit of the radio telescope caused by different loading cases was reported by Lösler et al. (2019). The commonly applied delay model requires a stable reference point, which is not affected by gravity-induced deformation (Nothnagel et al. 2019). Due to the mass of the receiving unit, deformation at the reference point cannot be excluded. A horizontal displacement Δ of the reference point position corresponds to a signal path variation $SPV = \frac{\Delta}{c_0}\cos(\varepsilon)$, where c_0 denotes the speed of light.

However, the analysis of the elevation-dependent experiments does not confirm this assumption. Fig. 6 depicts the observed horizontal variations Δx and Δy while the radio telescope was kept fixed in azimuth $\alpha = 90°$ and rotated up- and downwards about the elevation axis. Due to the higher uncertainty of the angle measurements, the noise of the derived Δx and Δy components are greater than for the vertical component Δz. Both series vary in a range of about 25 µm, which corresponds to a maximum signal path variation of less than 0.1 ps. However, the horizontal variations do not indicate a systematic behaviour that justifies a correction.

Large horizontal variation was unexpectedly observed when the radio telescope was rotated about the azimuth axis while the elevation axis remained fixed. As shown in Fig. 7, the position **E** varies by about ±250 µm. This variation is elevation-independent and reproducible at the elevation angles 5°, 45° and 90°. As shown in Fig. 1 and already mentioned, the SMR position **E** at end of the tube is ground-fixed and does not co-rotate about the azimuth axis. Instead of a gravity-induced deformation, it is more

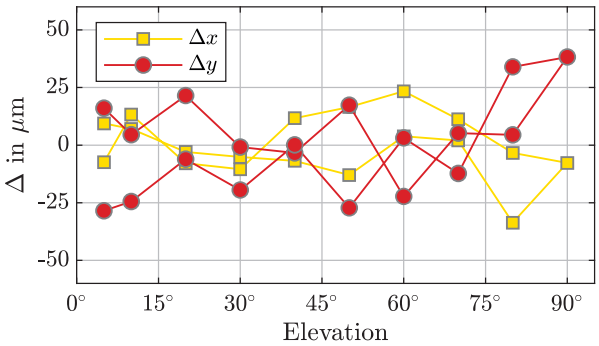

Fig. 6: Horizontal variation observed at the end of the tube **E** when the radio telescope was rotated up- and downwards about the elevation axis while the azimuth axis remains fixed at $\alpha = 90°$. Yellow squares and red circles relate to Δx and Δy, respectively.

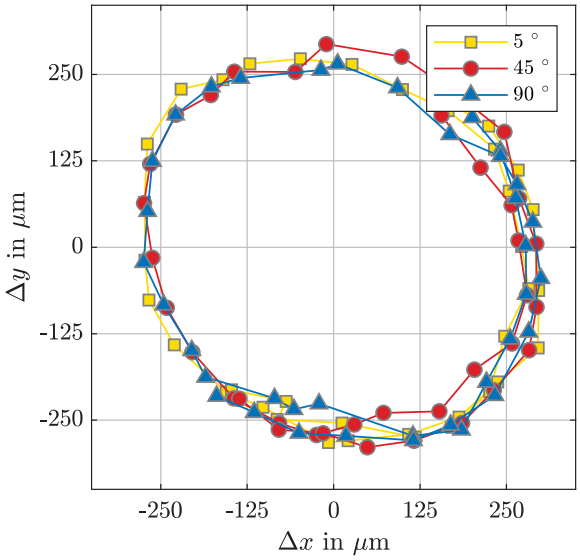

Fig. 7: Horizontal variation observed at the end of the tube **E** while the radio telescope was rotated about the azimuth axis in fixed elevations. Yellow squares, red circles, and blue triangles relate to the measurement series in elevation 5°, 45° and 90°.

likely that the end of the tube is forced by some asymmetrically arranged telescope components (cf. Eschelbach et al. 2025). During the rotation of the radio telescope, an azimuth-dependent load acts transversely to the tube. The bending of the tube leads to horizontal variation.

3.3 Tilt verification

For an independent verification of the results and to ensure that the cabin remains unaffected by the horizontal variation, inclination measurements were performed using an inclination sensor Nivel210 (Leica). The instrument is specified with a standard deviation of 50 $\frac{\mu m}{m}$ in a working range of ±3 $\frac{\mu m}{m}$.

The inclination sensor was positioned in place of the SMR at the end of the tube. Inclinations were observed in the fixed elevation position $\varepsilon = 90°$ while the radio telescope rotated about the azimuth axis from 0° to 360°. Fig. 8 depicts the observed inclinations. The data fit well with a circle having a radius of about 750 µm. The estimated residuals are quite small and scatter randomly. The observed inclination confirms the bending of the tube.

In order to compare the inclination measurement with the result of the laser tracker, the order of magnitude of the bending was estimated. In engineering mechanics, the bending B of an elastic structure such as a rod, which is unilateral clamped and subjected to a transversal load F, is readily derived from a third-degree polynomial, i. e.,

$$B(L) = A\left(\frac{L_0}{2}L^2 - \frac{1}{6}L^3\right). \tag{7}$$

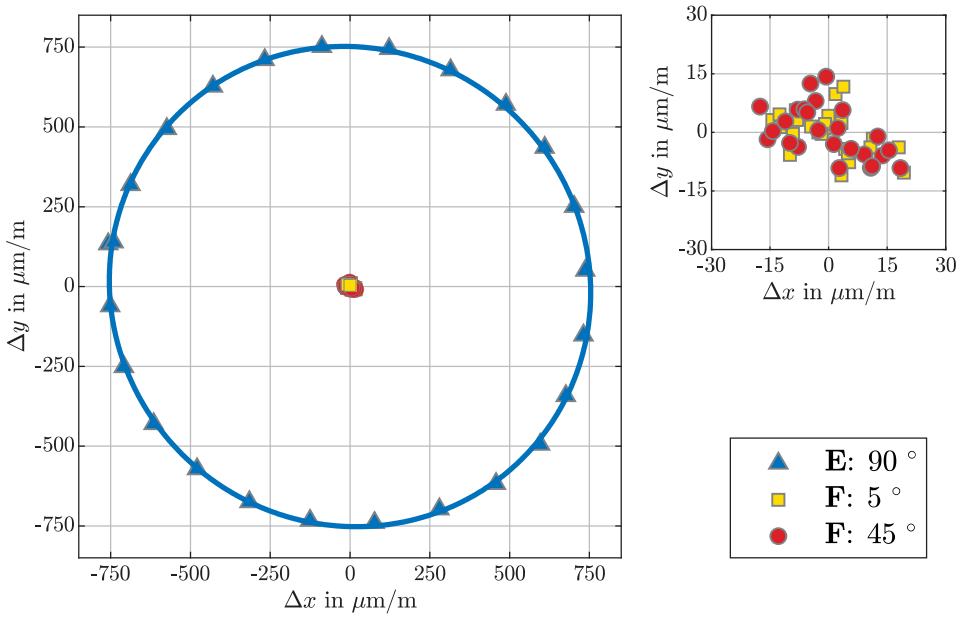

Fig. 8:
Observed inclinations when the radio telescope was rotated about the azimuth axis while the elevation remains fixed. Inclinations observed at the end of the tube E are shown in blue and were observed in $\varepsilon = 90°$. Inclinations observed on the cabin floor F are coloured yellow and red and refer to $\varepsilon = 5°$ and $\varepsilon = 45°$, respectively. A detailed plot depicts the series observed at F.

Here, $A = \frac{F}{E \cdot I}$ is the ratio between the acting load F and the bending stiffness $(E \cdot I)$, and L_0 is the length of the rod (Burg et al. 2011, p. 115). Assuming a transversal load at the end of the tube yields

$$A = -\frac{3B(L_0)}{L_0^3}. \tag{8}$$

The tilt δ of the rod results from the slope of the tangent, i. e.,

$$\tan(\delta(L)) = B'(L). \tag{9}$$

Based on blueprints of the radio telescope structure, the tube consists of several conical segments, which are screwed together. The length of the top segment of the tube is $L_0 = 50$ cm. The bending of the tube is taken from Fig. 7 and reads $B(L) = 250$ µm. According to (9), the tilt is $\delta(L_0) = 830 \frac{\mu m}{m}$. The remaining deviations of about 80 µm between the observed inclinations and the estimated tilt δ result from the model assumption used during the evaluation of (9). Nevertheless, the assumed bending of the tube and the order of magnitude are confirmed.

In order to evaluate whether the inclinations of the end of the tube can be transferred to the co-rotating azimuth cabin, which contains the reference point, inclination measurements were performed on the cabin floor. As the sensor co-rotated with the cabin, the observed changes in inclination Δx_i^α and Δy_i^α were converted to a ground-fixed frame using the corresponding azimuth angle α_i via

$$\begin{pmatrix} \Delta x_i \\ \Delta y_i \end{pmatrix} = \begin{pmatrix} \cos(\alpha_i) & \sin(\alpha_i) \\ -\sin(\alpha_i) & \cos(\alpha_i) \end{pmatrix} \begin{pmatrix} \Delta x_i^\alpha \\ \Delta y_i^\alpha \end{pmatrix}. \tag{10}$$

Fig. 8 depicts the performed inclination measurements at $\varepsilon = 5°$ and $\varepsilon = 45°$ in yellow and red, respectively. Unfortunately, the measurements at an elevation angle of 90° could not be analysed due to a registration error. The observed inclinations on the cabin floor are quite small compared to the inclinations measured at the end of the tube. As shown in the detailed plot, the series vary in a range of about $\pm 15 \frac{\mu m}{m}$ and, therefore, are less than the specified standard deviation of the sensor. In contrast to the tube, the cabin is not affected by a lateral load, and remains stable when the radio telescope rotates. For that reason, pointing errors of the radio telescope caused by a lateral load are unverifiable. However, the position at the end of the tube is unsuitable for a permanently installed measurement system for monitoring horizontal changes.

4 Conclusion

The backbone of almost all scientific investigation of the dynamic System Earth is a consistent global geodetic reference frame. Reference points realise the datum of such a global geodetic reference frame. Unstable reference points restrict the achievable accuracy and reliability and lead to misinterpretations. Wöppelmann and Marcos (2016) showed that the precision of currently established terrestrial reference frames limits our understanding of how sea level has changed in recent years and how future sea level might affect our lives. In order to meet further requirements, the Global Geodetic Observing System aims for a reference frame with an accuracy of 1 mm on a global scale (Blewitt et al. 2010). Investigation into the receiving unit of VLBI radio telescopes w. r. t. the pointing direction of the telescope indicates gravity-induced deformation. This deformation acts systematically but is correctable.

However, the commonly used delay model presumes a stable reference point (cf. Nothnagel et al. 2019). The reference points of VLBI radio telescopes are geometrically defined as the orthogonal projection of the secondary axis onto the primary axis. In order to determine the reference point, indirect approaches are required because the point is generally not physically realised. These approaches are almost insensitive to detect pointing-dependent variations and imply that the reference point is unaffected by load changes (e. g. Dawson et al. 2007, Lösler 2009, Bae and Hong 2022). Although almost all applications require an invariant position, detailed investigation on the pointing-dependent variation of the reference point does not exists so far.

In this contribution, the south-western VGOS radio telescope at the Onsala Space Observatory was studied in detail. The scope was to find a suitable substitute location, which allows a representative monitoring of the reference point's variation. Moreover, the magnitude of occurring deformation, in particular the pointing-dependent variation, should be examined in order to specify the required accuracy of the permanently installed measurement system. The geometric azimuth axis of the radio telescope under investigation runs through a hollow tube. This tube realises the ground-fixed part of the azimuth encoder, which is located at the end of the tube 10 m above the ground. The end of the tube is the closest position to the reference point in a ground-fixed frame, and is assumed to be a substitute location for a permanently installed measurement system. In order to monitor this position, a spherically mounted reflector was placed at the end of the tube and observed by a high-precise laser tracker AT960 via a plane mirror. Whereas elevation-dependent variation could not be detected, horizontal and vertical variations were observed while the radio telescope rotates about the azimuth axis. A large horizontal variation of about 250 µm was detected by the laser tracker, which results from a bending of the tube, caused by asymmetrically arranged telescope components. The bending was verified by additionally performed inclination measurements. In contrast to the tube, it was proven that the cabin is not tilted by a lateral load and remains stable. The position at the end of the tube is unsuitable for a permanently installed measurement system for monitoring horizontal changes. An azimuth-dependent vertical variation of about ±15 µm was detected at the end of the tube. This variation was confirmed by additional measurements at the support elements at the cabin and the cabin floor. One possible reason could be the unevenness of the gear rim realising the circular azimuth track, which is mounted on the top of the concrete monument. Furthermore, the end point of the tube was proven to be suitable to monitor the thermal expansion of the radio telescope. Compared with the thermal expansion as a result of daily or seasonal temperature changes, the observed vertical variation caused by the rim is quite small and only a second-order effect. Independently of the reason for the vertical variation, the end of the tube is suitable for a permanently installed measurement system for monitoring vertical changes. In order to reliably resolve the daily vertical variation a measurement accuracy of $\ll 100$ µm is recommended for an installed monitoring system.

Funding

This research project received funding from the Erna and Victor Hasselblad Foundation (Gothenburg).

References

Altamimi, Z., Rebischung, P., Collilieux, X., Métivier, L., Chanard, K. (2023): ITRF2020: an augmented reference frame refining the modeling of nonlinear station motions. J Geo, 97(5). DOI: 10.1007/s00190-023-01738-w.

Bae, T.-S., Hong, C.-K. (2022): Sphero-Conical Modeling for the Estimation of Very Long Baseline Interferometry Invariant Point. Sensors, 22(20), 7937. DOI: 10.3390/s22207937.

Blewitt, G., Altamimi, Z., Davis, J., Gross, R., Kuo, C.-Y., Lemoine, F. G., Moore, A. W., Neilan, R. E., Plag, H.-P., Rothacher, M., Shum, C. K., Sideris, M. G., Schöne, T., Tregoning, P., Zerbini, S. (2010): Geodetic Observations and Global Reference Frame Contributions to Understanding Sea-Level Rise and Variability. In: Church, J. A., Woodworth, P. L., Aarup, T., Wilson, W. S. (Eds.): Understanding Sea-Level Rise and Variability, Wiley-Blackwell, 256–284. DOI: 10.1002/9781444323276.ch9.

Burg, K., Haf, H., Wille, F., Meister, A. (2011): Höhere Mathematik für Ingenieure – Band I: Analysis, 9th ed, Springer, Wiesbaden. DOI: 10.1007/978-3-8348-9929-3.

Burge, J. H., Su, P., Zhao, C., Zobrist, T. (2007): Use of a commercial laser tracker for optical alignment. In: Sasian, J. M., Ruda, M. C. (Eds.): Optical System Alignment and Tolerancing, Vol. 6676, SPIE, 66760E. DOI: 10.1117/12.736705.

Charlot, P., Jacobs, C. S., Gordon, D., Lambert, S., de Witt, A., Böhm, J., Fey, A. L., Heinkelmann, R., Skurikhina, E., Titov, O., Arias, E. F., Bolotin, S., Bourda, G., Ma, C., Malkin, Z., Nothnagel, A., Mayer, D., MacMillan, D. S., Nilsson, T., Gaume, R. (2020): The third realization of the International Celestial Reference Frame by very long baseline interferometry. Astron Astrophys, 644(A159), 1–28. DOI: 10.1051/0004-6361/202038368.

Dawson, J., Sarti, P., Johnston, G. M., Vittuari, L. (2007): Indirect approach to invariant point determination for SLR and VLBI systems: an assessment. J Geo, 81(6-8), 433–441. DOI: 10.1007/s00190-006-0125-x.

Elgered, G., Carlsson, T. R. (1995): Temperature Stability of the Onsala 20-m Antenna and Its Impact on Geodetic VLBI. In: Lanotte, R., Bianco, G. (Eds.): Proceedings of the 10th European VLBI for Geodesy and Astrometry (EVGA) Working Meeting, 69–78.

Eschelbach, C., Lösler, M., Haas, R. (2025): Metrological Investigations on the Stability of Reference Points of VGOS Antennas. In: Behrend, D., Baver, K. D., Armstrong, K. L. (Eds.): Proceedings of the 13th IVS General Meeting, NASA/CP–20250002586, NASA, 97–103.

Foppe, K. Neitzel, F. (2014): Von der Zufallsgröße zur Trendschätzung im vermittelnden Ausgleichungsmodell. In: DVW e. V. (Ed.): Zeitabhängige Messgrößen – Ihre Daten haben (Mehr-)Wert. DVW-Schriftenreihe, Band 74, Augsburg, 35–64.

Gassner, G., Ruland, R. (2011): Instrument tests with the new Leica AT401. In: Proceedings of the 11th International Workshop on Accelerator Alignment (IWAA 2010), SLAC-PUB-14300, DESY. Hamburg, 1–5.

Gawronski, W., Baher, F., Quintero, O. (2000): Azimuth-track level compensation to reduce blind-pointing errors of the Deep Space Network antennas. IEEE Antennas Propag Mag, 42(2), 28–38. DOI: 10.1109/74.842123.

Gross, R., Beutler, G., Plag, H.-P. (2009): Integrated Scientific and Societal User Requirements and Functional Specifications for the

GGOS. In: Plag, H.-P., Pearlman, M. (Eds.): Global Geodetic Observing System – Meeting the Requirements of a Global Society on a Changing Planet in 2020, Springer, Berlin, 209–224. DOI: 10.1007/978-3-642-02687-4_7.

Guillory, J., Truong, D., Wallerand, J.-P., Lösler, M., Eschelbach, C., Mähler, S., Klügel, T. (2023): Determination of the reference point of a radio telescope using a multilateration-based coordinate measurement prototype. Precis Eng, 83, 69–81. DOI: 10.1016/j.precisioneng.2023.05.007.

Haas, R., Casey, S., Conway, J., Elgered, G., Hammargren, R., Helldner, L., Johansson, K.-Å., Kylenfall, U., Lerner, M., Pettersson, L., Wennerbäck, L. (2019): Status of the Onsala Twin Telescopes – Two Years After the Inauguration. In: Haas, R., García-Espada, S., Fernández, J. A. L. (Eds.): Proceedings of the 24th European VLBI for Geodesy and Astrometry (EVGA) Working Meeting, Centro Nacional de Información Geográfica (CNIG), 5–9. DOI: 10.7419/162.08.2019.

Hesch, J. A., Mourikis, A. I., Roumeliotis, S. I. (2008): Determining the camera to robot-body transformation from planar mirror reflections. In: IEEE/RSJ International Conference on Intelligent Robots and Systems, Vol. 2, 3865–3871. DOI: 10.1109/IROS.2008.4651121.

Heuneke, O., Kuhlmann, H., Welsch, W., Eichhorn, A. Neuner, H.-B. (2013): Auswertung geodätischer Überwachungsmessungen. In: Möser, M., Müller, G., Schlemmer, H. (Eds.): Handbuch Ingenieurgeodäsie, 2nd ed, Wichmann, Berlin.

ISO 10360-10 (2021): Geometrical product specifications (GPS) – Acceptance and reverification tests for coordinate measuring systems (CMS) – Part 10: Laser trackers. International Organization for Standardization (ISO).

Li, J., Zhang, J., Guo, L. (2013): On the monitoring model of reference point of VLBI antenna. Sci China-Phys Mech Astron, 56(10), 1987–1994. DOI: 10.1007/s11433-013-5171-9.

Li, N., Duan, B., Li, X., Zheng, B., Wu, J. (2022): A Reverse-Design Strategy for the Track Error of the Qi Tai Telescope Based on Pointing Accuracy. Engineering, 13, 209–216. 10.1016/j.eng.2021.11.015.

Li, N., Li, P., Wu, J., Duan, B.-Y. (2017): Modeling the rail surface unevenness of a high-precision radio telescope. Res Astron Astrophys, 17(3). DOI: 10.1088/1674-4527/17/3/23.

Lösler, M. (2009): New Mathematical Model for Reference Point Determination of an Azimuth-Elevation Type Radio Telescope. J Surv Eng, 135(4), 131–135. DOI: 10.1061/(asce)su.1943-5428.0000010.

Lösler, M. (2021): Modellbildungen zur Signalweg- und in-situ Referenzpunktbestimmung von VLBI Radioteleskopen. Deutsche Geodätische Kommission (DGK), Series C, No 865, Munich.

Lösler, M., Eschelbach, C., Klügel, T., Riepl, S. (2021): ILRS Reference Point Determination Using Close Range Photogrammetry. Appl Sci, 11(6). DOI: 10.3390/app11062785.

Lösler, M., Eschelbach, C., Schenk, A., Neidhardt, A. (2010): Permanentüberwachung des 20 m VLBI-Radioteleskops an der Fundamentalstation in Wettzell. zfv – Zeitschrift für Geodäsie, Geoinformatik und Landmanagement, 135(1), 40–48.

Lösler, M., Haas, R., Eschelbach, C. (2013): Automated and continual determination of radio telescope reference points with sub-mm accuracy: results from a campaign at the Onsala Space Observatory. J Geod, 87(8), 791–804. DOI: 10.1007/s00190-013-0647-y.

Lösler, M., Haas, R., Eschelbach, C. (2016): Terrestrial Monitoring of a Radio Telescope Reference Point Using Comprehensive Uncertainty Budgeting. J Geo, 90(5), 467–486. DOI: 10.1007/s00190-016-0887-8.

Lösler, M., Haas, R., Eschelbach, C., Greiwe, A. (2019): Gravitational Deformation of Ring-Focus Antennas for VGOS – First Investigations at the Onsala Twin Telescopes Project. J Geo, 93(10), 2069–2087. DOI: 10.1007/s00190-019-01302-5.

Mähler, S., Klügel, T., Lösler, M., Schüler, T., Plötz, C. (2019): Permanent Reference Point Monitoring of the TWIN Radio Telescopes at the Geodetic Observatory Wettzell. In: Armstrong, K. L., Baver, K. D., Behrend, D. (Eds.): Proceedings of the 10th IVS General Meeting 2018 – Global Geodesy and the Role of VGOS – Fundamental to Sustainable Development, NASA/CP–2019219039, 251–255.

Morse, E., Welty, V. (2015): Dynamic testing of laser trackers. CIRP Annals, 64(1), 475–478. DOI: 10.1016/j.cirp.2015.04.090.

Ning, T., Haas, R., Elgered, G. (2015): Determination of the local tie vector between the VLBI and GNSS reference points at Onsala using GPS measurements. J Geo, 89(7), 711–723. DOI: 10.1007/s00190-015-0809-1.

Nothnagel, A., Artz, T., Behrend, D., Malkin, Z. (2017): International VLBI Service for Geodesy and Astrometry: Delivering high-quality products and embarking on observations of the next generation. J Geo, 91(7), 711–721. DOI: 10.1007/s00190-016-0950-5.

Nothnagel, A., Holst, C., Haas, R. (2019): A VLBI delay model for gravitational deformations of the Onsala 20 m radio telescope and the impact on its global coordinates. J Geo, 93(10), 2019–2036. DOI: 10.1007/s00190-019-01299-x.

Pérez Muñoz, P., Albajez García, J. A., Santolaria Mazo, J. (2016): Analysis of the initial thermal stabilization and air turbulences effects on Laser Tracker measurements. J Manuf Syst, 41, 277–286. DOI: 10.1016/j.jmsy.2016.10.002.

Petrachenko, B., Niell, A., Behrend, D., Corey, B., Böhm, J., Charlot, P., Collioud, A., Gipson, J., Haas, R., Hobiger, T., Koyama, Y., MacMillan, D., Malkin, Z., Nilsson, T., Pany, A., Tuccari, G., Whitney, A., Wresnik, J. (2009): Design aspects of the VLBI2010 system. NASA/TM2009-214180.

Sovers, O. J., Fanselow, J. L., Jacobs, C. S. (1998): Astrometry and geodesy with radio interferometry: experiments, models, results. Rev Mod Phys, 70(4), 1393–1454. DOI: 10.1103/revmodphys.70.1393.

United Nations (2015): A global geodetic reference frame for sustainable development. Report of the Economic and Social Council. https://ggim.un.org/documents/a_res_69_266_e.pdf, last access May 30, 2025.

Wöppelmann, G., Marcos, M. (2016): Vertical land motion as a key to understanding sea level change and variability. Rev Geophys, 54(1), 64–92. DOI: 10.1002/2015rg000502.

Wresnik, J., Haas, R., Boehm, J., Schuh, H. (2006): Modeling thermal deformation of VLBI antennas with a new temperature model. J Geo, 81(6-8), 423–431. DOI: 10.1007/s00190-006-0120-2.

Xu, Q., Xue, F., Wang, H., Yi, L. (2023): Measurement and Correction of Pointing Error Caused by Radio Telescope Alidade Deformation based on Biaxial Inclination Sensor. In: Micromachines 14(7). DOI: 10.3390/mi14071283.

Zernecke, R. (1999): Seasonal variations in height demonstrated at the radio telescope reference point. In: Schlüter, W., Hase, H. (Eds.): Proceedings of the 13th European VLBI for Geodesy and Astrometry (EVGA) Working Meeting, 15–18.

Contact

Michael Lösler
Laboratory for Industrial Metrology, Faculty of Architecture, Civil Engineering and Geomatics, Frankfurt University of Applied Sciences
Nibelungenplatz 1, 60318 Frankfurt am Main, Germany
michael.loesler@fra-uas.de
ORCID: https://orcid.org/0000-0002-1979-263X

Cornelia Eschelbach
Laboratory for Industrial Metrology, Faculty of Architecture, Civil Engineering and Geomatics, Frankfurt University of Applied Sciences
Nibelungenplatz 1, 60318 Frankfurt am Main, Germany
cornelia.eschelbach@fra-uas.de
ORCID: https://orcid.org/0000-0003-4959-8712

Rüdiger Hass
Onsala Space Observatory, Department of Space, Earth and Environment, Chalmers University of Technology
439 92 Onsala, Sweden
rudiger.haas@chalmers.se
ORCID: https://orcid.org/0000-0003-2681-9228